

Importance of Volume Discretization of Single and Coupled Interconnects

Ahmed Shebaita
EECS Department, Northwestern
University
Evanston, IL 60208

Dusan Petranovic
Mentor Graphics,
San Jose, CA 95131

Yehea Ismail
EECS Department, Northwestern
University
Evanston, IL 60208

ABSTRACT

This paper presents figures of merit and error formulae to determine which interconnects require volume discretization in the GHz range. Most of the previous work focused mainly on efficient modeling of volume discretized interconnects using several integration and reduction techniques. However, little work has been done to characterize when using the simple DC model has an impact on critical circuit metrics such as delay, impedance ...etc. Most of the previous work simply assumes that when skin depth becomes smaller than the wire cross section dimensions, volume discretization becomes essential. However, careful analysis in this paper shows that this assumption is invalid and a figure of merit is derived to characterize when volume discretization of single and coupled wires is required. This derived figure of merit is shown to depend solely on the interconnect dimensions and spacing and is independent of the type of the materials used or technology scaling.

1. INTRODUCTION

A lot of work has been done to 3D model interconnects efficiently. Several models aim at finding inductance and resistance of interconnects as functions of frequency, e.g. [1]-[3]. Although these models are accurate, they are difficult to use with most available simulators [4]. Several other models try to find frequency independent lumped-element circuits to replace the original frequency dependent elements. Among these models are the volume filament model [5], compact circuit models [6], and the reduced decoupled R-L model [7]. For example, Figure 1 shows the volume filament model and its equivalent circuit. As can be seen, volume discretization makes circuit simulation very expensive, similar to any other technique to include the interconnect 3D models in circuit simulations even after using several reduction techniques. Therefore, it is very important to know when 3D models result in significantly different circuit behavior as compared to using the DC model.

Permission to make digital or hard copies of all or part of this work for personal or classroom use is granted without fee provided that copies are not made or distributed for profit or commercial advantage and that copies bear this notice and the full citation on the first page. To copy otherwise, to republish, to post on servers or to redistribute to lists, requires prior specific permission and/or a fee.

ICCAD'06, November 5-9, 2006, San Jose, CA
Copyright 2006 ACM 1-59593-389-1/06/0011...\$5.00

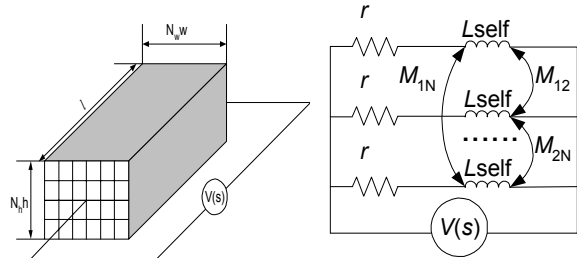


Figure 1: Rectangular interconnect 3D model

Most of the previous work assumes that using the 3D model leads to significant changes in the circuit performance when the operating frequency is high enough such that the skin depth starts to be comparable to the interconnect cross section dimensions. In such cases, the interconnect effective cross section area becomes less than that of the geometrical cross section as shown in Figure 2. This condition can be expressed mathematically as:

$$\Delta < 0.5 \min(w, t) \quad (1)$$

Where Δ is the skin depth and is given by

$$\Delta = \frac{1}{\sqrt{\pi f \mu \sigma}} \quad (2)$$

The critical frequency above which volume discretization becomes mandatory is given by:

$$f = \frac{4}{\min(w, t)^2 \mu \pi \sigma} \quad (3)$$

Based on (3), the frequency boundary after which the 3D model should be used is 4 GHz for an interconnect width of 2 μ m. Signal harmonics in current technologies far exceed 6 GHz and wires wider than 2 μ m are frequent in power and clock distribution networks and in global interconnect. Therefore, this metric has led to the conclusion that in current technologies, including volume discretization for on chip interconnects is essential

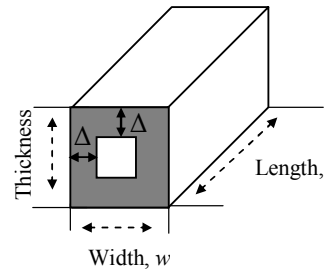


Figure 2: Effective cross sectional area of a rectangular interconnect under skin effect

This conclusion, despite being widely used, is not correct. This boundary was chosen based on the fact that when skin depth starts to be less than the interconnect cross section, the resistance starts to increase significantly and the DC model is expected to be erroneous. However, at such high frequencies the inductive impedance dominates the total impedance and inductance is practically constant independent of frequency.

The analysis presented in this paper starts by deriving a figure of merit that characterizes when volume discretization of the wires is required. This figure of merit is derived based on the behavior of both the resistive and inductive impedances over the entire frequency range. The study shows that simply using the DC model of the wire leads to minimal error at most wires dimensions and spacing.

The rest of the paper is organized as follows. The qualitative behavior of interconnect impedance at high frequency is studied in section 2. The derivation of the figure of merit that characterizes the importance of volume discretization for a single wire and the simulation results that verifies the proposed figure of merit are presented in section 3. The single wire case is studied in details to gain intuitive understanding of the behavior of filamented interconnects. Section 4 presents the derivation of a modified figure of merit that includes the effect of coupling and loop inductance. The simulation results that verify the figure of merit are also presented in section 4. The Formulations that quantify the error introduced by using DC model instead of an accurate model with volume filamentations are presented in section 5. Finally, the paper is concluded in section 6

2. QUALITATIVE BEHAVIOR OF INTERCONNECT IMPEDANCE UNDER SKIN EFFECT

The behavior of the resistance and inductance with frequency for a rectangular interconnect is studied based on the volume discretized 3D model shown in **Figure 1**. The interconnect is divided into $N_l \times N_w$ filaments such that the cross section dimension of each filament is significantly smaller than the skin depth. This discretization ensures that the current is approximately constant within each filament.

The simulation results for the resistance and inductance of a typical interconnect are shown in Figure 3. These results match well the resistance and inductance formulae derived in [10]-[14]. Note that the resistance changes significantly while the inductance is practically constant over the entire frequency range.

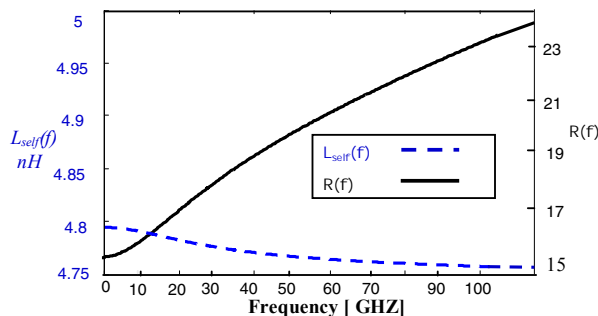


Figure 3: Resistance and inductance behavior with frequency

In the low frequency region where the skin depth is larger than the wire cross section, both the inductance and the resistance are practically constant, and equal to their DC values. At this frequency region, the resistance dominates the impedance but has a very low rate of change, which means that skin effect is negligible in this

frequency region. Thereafter, at higher frequencies, the skin depth becomes comparable to the wire cross section and the current starts to concentrate along the perimeter of the wire cross section, increasing the resistance. This current concentration also modifies the magnetic field in the space between the conductors and within each conductor resulting in a slight variation of the total inductance. At higher frequencies, the inductive impedance starts to dominate the total impedance as shown in Figure 4, and the inductance becomes practically constant. At even higher frequencies the resistance increases as the square root of frequency while the inductive impedance increases as frequency. Thus, the inductive impedance further dominates the total impedance.

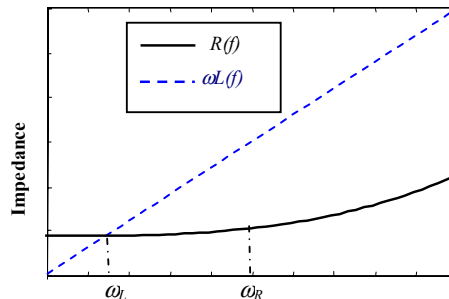


Figure 4: The behavior of $R(f)$ and $\omega L(f)$

The skin impedance can be described in terms of two key frequency points as shown in Figure 4. The first frequency point ω_L is the frequency at which the inductance starts to dominate the total impedance. The second frequency point ω_R is the frequency at which the resistance starts to increase with a high rate (when skin depth becomes comparable to the wire cross section dimensions).

Both ω_L and ω_R are functions of the interconnect dimensions. In cases when ω_R is bigger than ω_L , the impedance is always dominated by a slowly varying element with frequency, i.e. the impedance dominant term is always the one whose DC model has minimal error. This behavior occurs because the frequency region at which the resistance starts to increase at a high rate has the inductive impedance as the dominant factor and the inductance is practically constant in that range.

3. THE IMPORTANCE OF VOLUME DISCRETIZATION FOR A SINGLE WIRE

In this section, the figure of merit that characterizes when volume discretization becomes important for a single wire is derived and the experimental results are shown to verify its correctness. Section 3.1 shows that for a single wire case, the DC model of an interconnect can be used with minimal error if the ratio between the interconnect length, l , to the summation of its width, w , and thickness, t , is greater than 7. Section 3.2 explores the error in the total impedance Z_{DC} versus $Z_{3D}(f)$ as a function of wire dimensions. Section 3.3 presents the error in delay introduced by using the DC model instead of the 3D model for different values of $\frac{l}{w+t}$. The effect of scaling the interconnect dimensions, while having a constant $\frac{l}{w+t}$ is studied in section 3.4.

3.1 Figure of Merit for a Single Wire

Volume discretization can be considered to be of minimal importance under the interconnect dimension conditions that makes $\omega_R \gg \omega_L$. Based on simulation results and theoretical analysis, as will be shown in subsequent sections, less than 5% error is guaranteed under the interconnect dimensions conditions that makes $\omega_R > 5 \omega_L$.

The frequency point ω_L occurs when the inductive impedance value equals that of the resistance. Thus, ω_L is given by:

$$\omega_L = \frac{R}{L} \quad (4)$$

If ω_R is greater than 5 times ω_L , this intersection point occurs when the resistance is almost at its DC value as shown in Figure 5. Note also that inductance is almost constant. Hence, the DC values of the resistance and inductance are used in (4). The DC value of the resistance is given by

$$R_{DC} = \frac{l}{\sigma wt} \quad (5)$$

where σ is the wire conductivity. The DC inductance is [7-11]

$$L_{DC} \approx \frac{\mu}{2\pi} l \left(\ln\left(\frac{2l}{w+t}\right) + 0.5 + 0.2235\left(\frac{w+t}{l}\right) \right) \quad (6)$$

where μ is the magnetic permeability of SiO₂. Hence, ω_L is given by

$$\omega_L \approx \frac{\frac{l}{\sigma wt}}{\frac{\mu}{2\pi} l \left(\ln\left(\frac{2l}{w+t}\right) + 0.5 + 0.2235\left(\frac{w+t}{l}\right) \right)} \quad (7)$$

Simplifying (7) yields,

$$\omega_L = \frac{2\pi}{\mu \sigma wt \left(\ln\left(\frac{l}{w+t}\right) + 1.2 + 0.2235\left(\frac{w+t}{l}\right) \right)} \quad (8)$$

The frequency point ω_R occurs when the skin depth is equal to half the minimum of the interconnect width and thickness as shown in Figure 2. Hence, ω_R can be calculated from,

$$\frac{1}{\sqrt{\pi f \mu \sigma}} = 0.5 \min(w, t) \quad (9)$$

$$\omega_R = \frac{8}{\min(w, t)^2 \mu \sigma} \quad (10)$$

Substituting in the condition $\omega_R > 5 \omega_L$ results in

$$\ln\left(\frac{l}{w+t}\right) + 0.2235\left(\frac{w+t}{l}\right) \geq \frac{1.9 \times \min^2(w, t)}{w \times t} \quad (11)$$

Since $\frac{\min^2(w, t)}{w \times t}$ is less than 1, the skin effect is negligible if

$$\ln\left(\frac{l}{w+t}\right) + 0.2235\left(\frac{w+t}{l}\right) \geq 1.9 \quad (12)$$

The minimum value of $\frac{l}{w+t}$ that satisfies (12) can be obtained graphically by finding the minimum value u at which the function $f(u) = \ln u + 0.2235\left(\frac{1}{u}\right)$ exceeds 1.9 as shown in Figure 5.

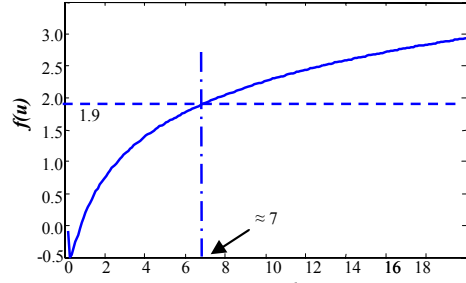


Figure 5: The minimum $\frac{l}{w+t}$ that results in no skin

The minimum value of $\frac{l}{w+t}$ that satisfies (12) is approximately 7. Hence, using the DC model of a single wire gives minimal error at any frequency if:

$$\frac{l}{w+t} \geq 7 \quad (13)$$

However, to prove the uniqueness of this value, the function $f(u)$ should be monotonically increasing for any $u \geq 7$. Differentiating $f(u)$ yields,

$$\frac{\partial f(u)}{\partial u} = \frac{1}{u} - \frac{0.2235}{u^2} \quad (14)$$

The condition for the function $f(u)$ to be monotonically increasing is, $\frac{\partial f(u)}{\partial u} > 0$, or,

$$\frac{1}{u} - \frac{0.2235}{u^2} > 0 \quad (15)$$

This condition is always satisfied for any $u > 0.2235$, which proves the uniqueness of the figure of merit defined in (13).

Note that the condition that ω_R is greater than 5 times ω_L can also be interpreted as the condition that makes the inductive impedance 5 times larger than the resistance at ω_R , the point at which the resistance starts to increase.

$$\omega_R > 5 \omega_L \Leftrightarrow \omega_R > 5 \frac{R}{L} \Leftrightarrow \omega_R L > 5 R \quad (16)$$

3.2 Error in Impedance Due to Using a DC Model

Figure 6-a shows the complete 3D model of an interconnect, while Figure 6-b shows the DC model of the same interconnect.

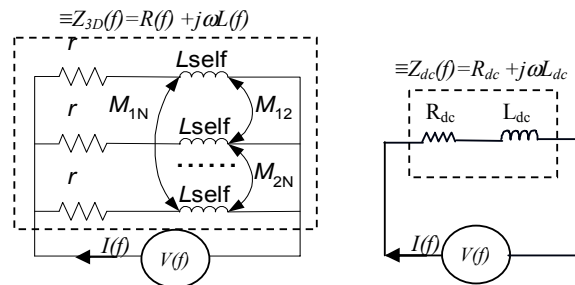


Figure 6 a: Complete 3D Model

b: DC Model

According to our figure of merit, skin effect is not important at any frequency when $\frac{l}{w+t} \geq 7$. When this condition is satisfied, the 3D impedance of the wire should be the same as the DC impedance at any frequency. The equivalence of these two impedances can be expressed as:

$$\left| \frac{Z_{3D}(f)}{Z_{DC}(f)} \right| = \frac{\sqrt{R^2(f) + (\omega L(f))^2}}{\sqrt{R_{DC}^2 + (\omega L_{DC})^2}} \cong 1 \quad (17)$$

$$\tan^{-1}\left(\frac{\omega L(f)}{R(f)}\right) - \tan^{-1}\left(\frac{\omega L_{DC}}{R_{DC}}\right) \cong 0 \quad (18)$$

Five cases are studied assuming $w=t=2.5 \mu\text{m}$ in each case. The interconnect length is varied such that $\frac{l}{w+t}$ varies between 10 - 40. Figure 7 shows the error in the impedance magnitude versus frequency. The phase error is shown in Figure 8. From Figure 7 and Figure 8, the entire frequency range can be divided into four main regions. In region I where $\omega < \omega_R$, the error increases monotonically at a slow rate. This increase is mainly due to the increase in the resistance value. In region II where $\omega_L < \omega < \omega_R$, the inductance starts to dominate the impedance, and the resistance is still changing slowly with frequency. Thus, the error rate, and eventually the error value decreases. In region III $\omega_R < \omega < 2\omega_R$. This is the region with the highest error rate. In this region the rate of change of resistance with frequency attains its maximum. However, the error is still small because the ratio between the inductive impedance and the resistance increases at a higher rate. In region IV where $2\omega_R < \omega$ the inductive impedance is dominating the total impedance, which leads to a significant decrease in the error rate since the inductance is very slowly varying with frequency.

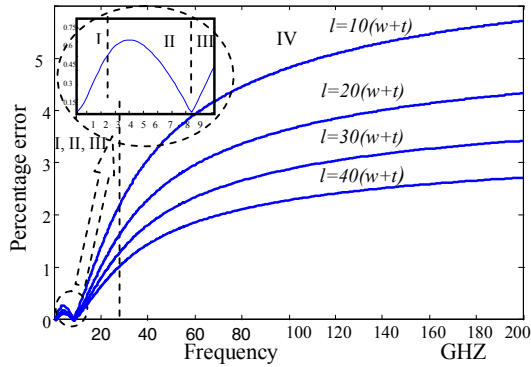


Figure 7: Percentage errors in impedance magnitude due to using the DC model

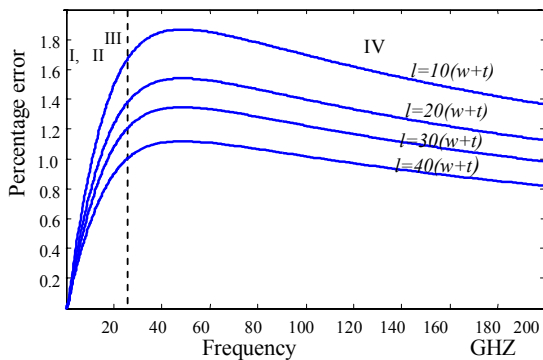


Figure 8: Percentage errors in phase due to using the DC model

3.3 Delay Error in Using the Interconnect DC Model Versus the 3D model

The experimental setup used in examining the impact of using interconnect DC model on delay is shown in Figure 9.

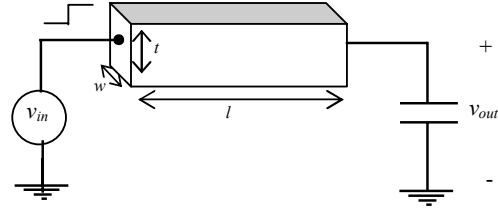


Figure 9: Delay experimental setup

The error in delay when an interconnect is modeled using the DC impedance instead of the complete 3D volume impedance is studied for different values of $\frac{l}{w+t}$. The interconnect shown in Figure 9 has $l=w=2 \mu\text{m}$, and the input source is a step input with slope of less than 0.01 ns, which includes very high frequency components. The output voltages at two interconnects having $\frac{l}{w+t}$ equals to 1 and 3 are shown in Figure 10 (a) and (b), respectively, and show errors of at least 50% in the output signal delay for low $\frac{l}{w+t}$. Also, the 3D model behaves more as an RC interconnect while the DC model tends to behave as an RLC circuit. This behavior is due to the increase in the resistance value of the 3D model due to skin effect. However, this difference between the two models is negligible for $\frac{l}{w+t} > 7$ as shown in Figure 10 (c) and (d). The delay error is less than 1% for $\frac{l}{w+t} > 7$. In addition, the DC model of the interconnect captures the signal waveform shape of the 3D model with negligible error.

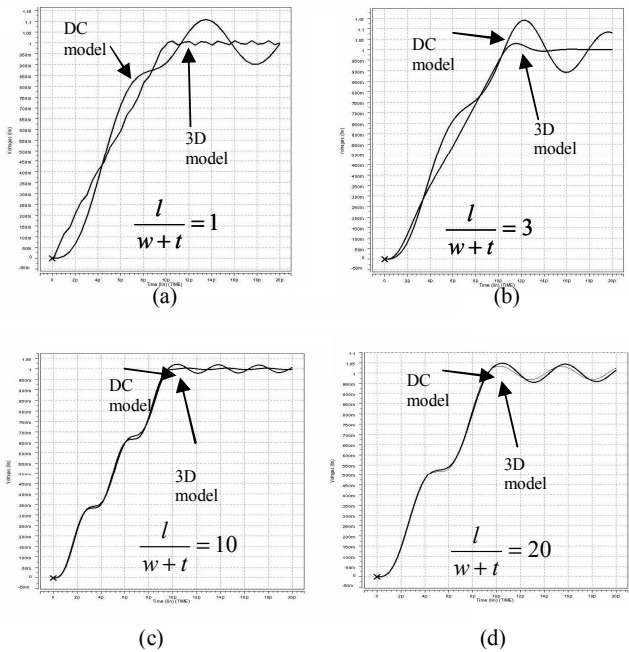


Figure 10: Delay error between DC model and 3D model for different $\frac{l}{w+t}$

3.4 Effect of Scaling the Interconnect Dimensions

The figure of merit introduced in section 3 predicts that scaling the interconnect dimensions does not affect the impact of skin effect as long as $\frac{l}{w+t}$ remains constant. Table 1 shows the percentage error in the total impedance magnitude and phase due to using the DC model instead of the 3D model for different interconnects with square shape cross sections.

Table 1: Percentage error in the total impedance magnitude and phase due to using the DC model instead of the 3D model

| | % error in magnitude | | | | %error in phase | | | |
|-------------|----------------------|-------------|-------------|-------------|-----------------|-------------|-------------|-------------|
| | $w=1 \mu m$ | $w=2 \mu m$ | $w=3 \mu m$ | $w=4 \mu m$ | $w=1 \mu m$ | $w=2 \mu m$ | $w=3 \mu m$ | $w=4 \mu m$ |
| $l=5(w+t)$ | 7.5 | 7.25 | 6.6 | 6.8 | 2.5 | 2.2 | 2.2 | 2.3 |
| $l=10(w+t)$ | 5.9 | 6.27 | 5.75 | 5.8 | 1.8 | 1.8 | 1.77 | 1.73 |
| $l=15(w+t)$ | 5.4 | 5.43 | 5.36 | 5.41 | 1.55 | 1.48 | 1.47 | 1.52 |
| $l=20(w+t)$ | 4.9 | 4.88 | 4.89 | 4.9 | 1.44 | 1.44 | 1.44 | 1.44 |
| $l=25(w+t)$ | 4.7 | 4.7 | 4.7 | 4.7 | 1.3 | 1.3 | 1.3 | 1.3 |
| $l=50(w+t)$ | 3.4 | 3.4 | 3.4 | 3.4 | 0.8 | 0.8 | 0.8 | 0.8 |

The experimental results presented in Table 1 shows that the percentage error in both impedance magnitude and phase is not varying with scaling the interconnect dimensions while having constant $\frac{l}{w+t}$ which verifies the independence of the figure of merit of absolute interconnect dimensions.

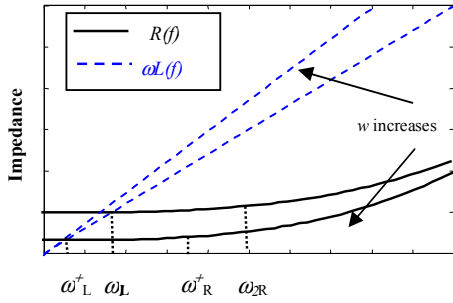


Figure 11: The change in ω_L and ω_R with $\frac{l}{w+t}$

The physical explanation of this trend for a constant aspect ratio is that increasing the length, width, and thickness of the interconnect such that $l/(w+t)$ is kept constant decreases the frequency point ω_R since the skin depth becomes comparable to the wire width at lower frequencies. However, this scaling in the wire dimensions decreases the resistance and at the same time increases the inductive impedance. Thus, the frequency point ω_L decreases as well. Figure 11 shows the behavior of the two frequency point with increasing the interconnect dimensions while having a constant $\frac{l}{w+t}$.

Figure 12 shows the resulting ω_L and ω_R when applying the complete 3-D model simulation to different interconnects having square shape cross section. Note that the intersection point is at the same $\frac{l}{w+t}$ which agrees very well with our metric.

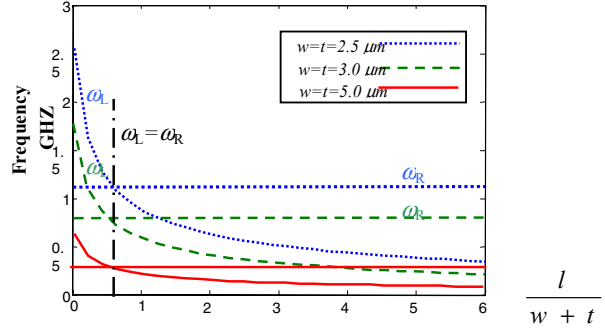


Figure 12: The behavior of ω_L and ω_R for Different Interconnect Widths

4. IMPORTANCE OF VOLUME DISCRETIZATION FOR COUPLED WIRES

In this section, the figure of merit that characterizes when volume discretization becomes important for coupled wires is derived and the experimental results are shown to verify its correctness. Section 4.1 shows the impact of coupling on the interconnect circuit behavior. The modified figure of merit that includes the effect of inductive coupling in characterizing the importance of volume discretization is derived in section 4.2. Section 4.3 shows the experimental results that verifies the figure of merit.

4.1 Impact of Inductive Coupling

Inductive coupling results in transfer of energy from one circuit component to another through the shared magnetic field. Inductive coupling effect diminishes as distance between wires increases. In the extreme situation where wires are far apart, the inductive coupling between wires become negligible and the figure of merit that characterize the relevance of volume discretization derived in the previous section can be applied to each wire. However, measures must be taken to handle inductive coupling when it becomes significant.

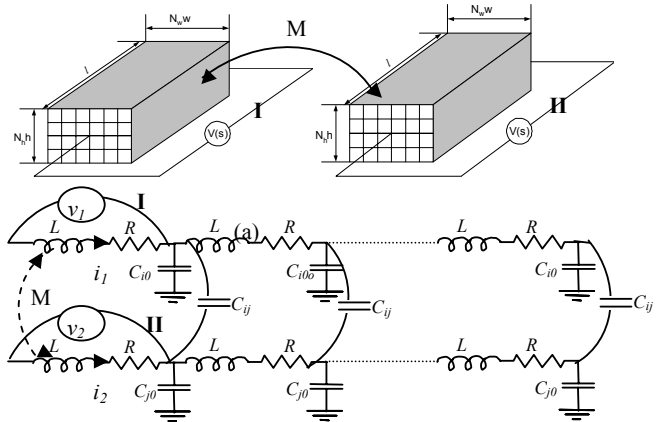


Figure 13: Interconnects with proximity effects (mutual coupling)

Figure 13 (a) illustrates two coupled interconnects by a mutual inductance M . The equivalent circuit of the two interconnects shown in Figure 13 (a) is illustrated in Figure 13. Because of coupling, the equation of each circuit contains a term depending on the current change in the other circuit as shown in (19).

$$\begin{aligned} v_1 &= i_1 R + L \frac{\partial i_1}{\partial t} + M \frac{\partial i_2}{\partial t} \\ v_2 &= i_2 R + L \frac{\partial i_2}{\partial t} + M \frac{\partial i_1}{\partial t} \end{aligned} \quad (19)$$

Thus, (19) can be analyzed based on three different possible cases of wire switching.

Case 1

In this case, it is assumed that there is no change in i_2 , while i_1 is following a unit step change in the voltage source v_1 . In this case (19) can be rewritten as:

$$\begin{aligned} v_1 &= i_1 R + L \frac{\partial i_1}{\partial t} + M \times 0 \\ v_2 &= i_2 R + L \times 0 + M \frac{\partial i_1}{\partial t} \end{aligned} \quad (20)$$

This case simply falls back to a single wire case and the previous figure of merit is valid

Case 2

In this case, it is assumed that the two wires switch similarly, resulting in a change in both i_2 and i_1 in the same direction. In this case (19) can be rewritten as:

$$\begin{aligned} v_1 &= i_1 R + (L + M) \frac{\partial i_1}{\partial t} \\ v_2 &= i_2 R + (L + M) \frac{\partial i_2}{\partial t} \end{aligned} \quad (21)$$

For this case, using the DC model for the wires results in even less error than the single wire case. This behavior is due to the increase in the effective inductance value which leads to a corresponding decrease in the frequency point ω_L . Thus, the figure of merit in (13) is also valid as an upper bound for this case

Case 3

In this case, the two wires switch oppositely, resulting in a change in both i_1 and i_2 but in opposite directions. In this case (19) can be rewritten as:

$$\begin{aligned} v_1 &= i_1 R + (L - M) \frac{\partial i_1}{\partial t} \\ v_2 &= i_2 R + (L - M) \frac{\partial i_2}{\partial t} \end{aligned} \quad (22)$$

This case results in a decrease in the total inductance value which leads to an increase in the frequency point ω_L . Hence, the figure of merit for a single wire should be modified to include the effect of mutual inductance when wires switch in opposite directions. Note that this case is equivalent to using the loop inductance.

4.2 Volume Discretization Figure of Merit in Case of Loop Inductance (case 3)

Inductive coupling affects the volume discretization figure of merit derived in the previous section in the case of oppositely switching interconnects. The total inductance is reduced to $L-M$. Thus, the frequency point ω_L should be redefined as:

$$\omega_L = \frac{R(f)}{L(f) - M(f)} \quad (23)$$

Denoting the distance between the center axes of the interconnects by d , M is given by [7-11]

$$M \approx \frac{\mu}{2\pi} l \left(\ln \left(\frac{l}{d} + \sqrt{1 + \frac{l^2}{d^2}} \right) - \sqrt{1 + \frac{d^2}{l^2}} + \frac{d}{l} \right) \quad (24)$$

For inductively coupled interconnects, ω_R is given by

$$\omega_R = \frac{8}{w^2 \mu \sigma} \quad (25)$$

Substituting in the condition $\omega_R > 5\omega_L$ yields

$$g(\alpha, \beta) = \ln(\alpha) + \frac{0.235}{\alpha} - \ln(\beta + \sqrt{1 + \beta^2}) + \sqrt{1 + \frac{1}{\beta^2}} - \frac{1}{\beta} - 1.9 \frac{w}{t} \geq 0 \quad (26)$$

where $\alpha = \frac{l}{w+t}$ and $\beta = \frac{l}{d}$. Figure 16 shows the plot of (26) at $w=t$, for different values of α and β . Figure 14 shows the values of α and β at which (26) is satisfied.

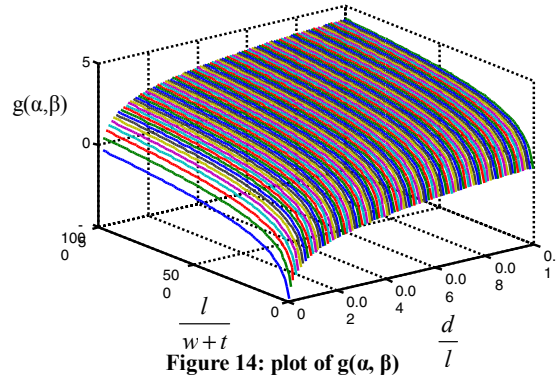


Figure 14: plot of $g(\alpha, \beta)$

It is shown in Figure 14 that there exist certain interconnect dimensions and spacing at which the interconnect DC model can be used with high accuracy.

The general figure of merit in terms of the interconnects dimensions that determines the importance of volume discretization in case of prominent inductive coupling can be obtained by applying curve fitting to (26) and is given by

$$\frac{l}{w+t} - 0.83 \frac{l}{d} > 2.7 e^{-\frac{w}{t}} \quad (27)$$

For $w=t$, the figure of merit reduces to

$$\frac{l}{w+t} - 0.83 \frac{l}{d} > 7 \quad (28)$$

4.3 Experimental Results for Delay Error

The experimental setup used in examining the delay error that results when using the DC model versus the 3D model is shown in Figure 15.

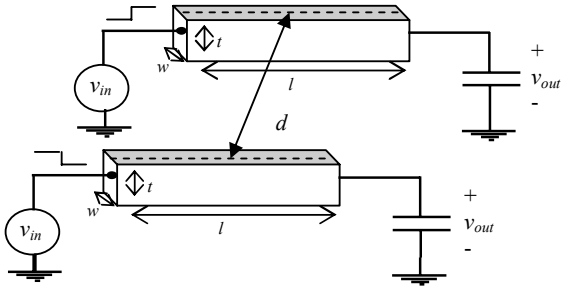


Figure 15: Delay experimental setup

The error in delay is studied for different values of l, w, t , and d . Figure 16 (a) shows the error in delay at aspect ratio = 1, $\frac{l}{w+t} = 10$ and $\frac{d}{l} = 0.0625$. This error is significantly reduced when the aspect ratio changes from 1 to 0.5 as shown in Figure 16(b). The reduction in delay error when increasing the wire spacing, d , and increasing $\frac{l}{w+t}$ are shown in Figure 16(c) and Figure 16(d), respectively. Figure 16 shows very small error even at the edge of the figure of merit. This is because of the capacitive effect which filters out the high frequency components. Hence, our figure of merit is conservative.

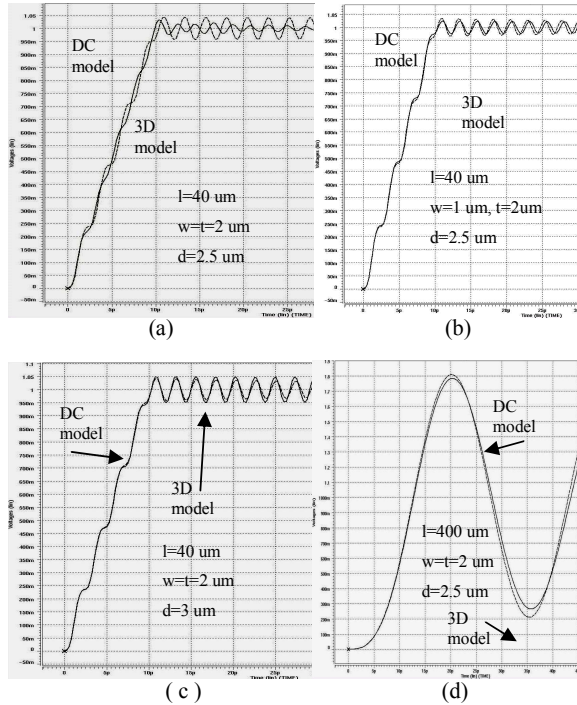


Figure 16: Delay error between DC model and volume discretized model for different wire dimensions

5. ERROR FORMULATION

The error that might arise in using the DC model of an interconnect is mainly due to the change of the resistance and mutual inductance from their DC values. Thus, there are two types of errors, the resistance error, E_R , and the mutual inductance error, E_M .

The resistance error arises due to the change in the effective value of the interconnect cross sectional area at frequencies higher than ω_R . Thus, the resistance error is only valid for operating frequencies $\omega > \omega_R$ and can be given by

$$E_R = \frac{R(f) - R_{DC}}{R(f)} = 1 - \frac{A_{eff}}{A_{DC}} \quad (29)$$

$$= 1 - \frac{2\Delta(w+t-2\Delta)}{wt}$$

Substituting from (2) into (29) yields

$$E_R \cong 1 - 2 \left(1 - \frac{1}{2} \sqrt{\frac{\omega_R}{\omega}} \right) \sqrt{\frac{\omega_R}{\omega}} \quad (30)$$

The error as presented in (30) is a tight upper bound assuming the resistance is completely dominating the total impedance. The relative change in the total impedance due to the relative change in the resistance can be derived by

$$\frac{\partial Z}{\partial R} = \frac{R}{\sqrt{R^2 + (\omega L_{eff})^2}} \Rightarrow \frac{\partial Z}{Z} = \frac{\partial R}{R} \frac{R^2}{R^2 + (\omega L_{eff})^2} \quad (31)$$

Substituting from (30) into (31), the effective error in the total impedance due to the resistance change can be given by

$$\hat{E}_Z^R \cong \left[1 - 2 \left(1 - \frac{1}{2} \sqrt{\frac{\omega_R}{\omega}} \right) \sqrt{\frac{\omega_R}{\omega}} \right] \frac{R^2}{R^2 + (\omega L_{eff})^2} \quad (32)$$

The mutual inductance error arises from the change in the effective distance between the centre axes of the interconnects, d , from being $s+w$ at low frequencies to approximately $s+\Delta$ at high frequencies, where s is the interconnect-to-interconnect spacing. Hence, the mutual inductance error, E_M , can be given by

$$E_M = \frac{M(f) - M_{DC}}{M(f)} \approx 1 - \frac{\ln\left(\frac{2l}{s+w}\right)}{\ln\left(\frac{2l}{s+\Delta}\right)} \quad (33)$$

$$= \frac{1}{\ln\left(\frac{2l}{d}\right)} \ln\left(\frac{s+w}{s+\Delta}\right)$$

Substituting from (2) into (33) yields

$$E_M = \frac{1}{\ln\left(\frac{2l}{d}\right)} \ln\left(\frac{s+w}{s + \frac{1}{2} w \sqrt{\frac{\omega_R}{\omega}}}\right) \quad (34)$$

The relative change in the total impedance due to the relative change in the mutual inductance can be derived by

$$\left| \frac{\partial Z}{\partial M} \right| = \left| \frac{\omega^2 L_{eff}}{\sqrt{R^2 + (\omega L_{eff})^2}} \right| \Rightarrow \left| \frac{\partial Z}{Z} \right| = \left| \frac{\partial M}{M} \frac{\omega^2 L_{eff} M}{R^2 + (\omega L_{eff})^2} \right| \quad (35)$$

Substituting from (34) into (35) gives the effective error in the total impedance due to the change in the mutual inductance as

$$\hat{E}_Z^M = \frac{1}{\ln\left(\frac{2l}{d}\right)} \ln\left(\frac{s+w}{s + \frac{1}{2}w\sqrt{\frac{\omega R}{\omega}}}\right) \frac{\omega^2 L_{eff} M}{R^2 + (\omega L_{eff})^2} \quad (36)$$

It can be deduced from (32) and (36) that an upper bound for the total error due to skin effect can be given by

$$\hat{E}_Z^{total} = \hat{E}_Z^R + \hat{E}_Z^M \quad (37)$$

It has to be mentioned here that (37) can be used to estimate the error in using the DC model of an interconnect whether or not the figure of merit in (13) or (27) is satisfied.

The figures of merit insure that at frequencies above ω_R when (32) becomes applicable, the value of the inductive impedance is at least 5 times that of the resistance which in turn results in negligible values for the resistance error at any frequency. In addition, to satisfy (27), the ratio between d and $w+t$ should be

$$d > 0.83(w+t) \quad (38)$$

This condition sets a minimum value for s to be comparable to the interconnect cross section dimension. Also the figure of merit in (27) sets a minimum value for the ratio between the interconnect length and its cross section dimensions. With these limitations, the error in (36) will also be negligible at any frequency. An example of $s=w=t$, the figure of merit in (27) deduce that l should be at least 70 times higher than the interconnect cross sectional dimensions. Substituting by these values in (36) would give an error that is less than 10% at frequencies higher than 100 GHZ. Hence, the satisfaction of the figures of merit implies that the total error in (37) is negligible.

6. CONCLUSION

The paper characterized the relevance of volume discretization in the GHZ range. It is shown that comparing the skin depth to the interconnect cross section dimensions cannot solely identify when to use volume discretization. A figure of merit that characterizes the importance of volume discretization for a single wire was then derived based on both the frequency point at which the skin depth starts to be comparable to the interconnect cross section dimensions and the frequency at which the resistance starts to have negligible impact on the total impedance. The experimental results verified the figure of merit in terms of both the signal delay error and total interconnect impedance error. Moreover, it was shown that the variation of other parameters such as scaling of interconnect dimensions and having different physical constants do not have any impact on the introduced error which agrees with the prediction of the figure of merit. The impact of coupling on determining the importance of volume discretization is studied. A modified figure of merit was also derived that includes the inductive coupling effect. The experimental results also verified the modified figure of merit. Finally, error formulae that quantifies the error in using the DC model of an interconnect were derived

7. REFERENCES

- [1] K. M. Coperich and A. E. Ruehli, "Enhanced skin effect for partial-element equivalent-circuit (PEEC) models," *IEEE Transactions on Microwave Theory and Techniques*, vol. 48, pages 1435-1442, 2000.
- [2] M. Xu and L. He, "An efficient model for frequency dependent on-chip inductance," *Proceedings of the 2001 conference on Great Lakes symposium on VLSI*, pages 115-12, 2001.
- [3] M. J. Tsuk and A. J. Kong, "A hybrid method for the calculation of the resistance and inductance of transmission lines with arbitrary cross sections," *IEEE Transactions on microwave Theory and Techniques*, vol. 39, pages 1338-1347, 1991.
- [4] P. Silvester, "Modal network theory of skin effect in flat conductors," *Proceedings of the IEEE*, vol. 54, pages 1147-1151, 1966.
- [5] H. A. Wheeler "Formulas for the skin effect". *Proceeding of the institute of radio engineers*, vol. 30, pages 412-424, 1942.
- [6] S. Kim and D. P. Neikirk, "Compact equivalent circuit model for the skin effect," *1996 IEEE-M7T-S International Microwave Symposium*, San Francisco, June 1996.
- [7] S. Mei and Y. I. Ismail, "Modeling skin and proximity effect with the reduced realizable RL circuits", *IEEE Transactions on Very 00000Large Scale Integration Systems (TVLSI)*, vol. 12, no. 4, pp. 437-447, April 2004.
- [8] B. Krauter and S. Mehrotra, "Layout based frequency dependent inductance and resistance extraction for on-chip interconnect timing analysis," *Proceedings of DAC*, pages 303-308, 1998.
- [9] B. E. Keiser, *Principles of Electromagnetic Compatibility*. Norwood, MA: Artech House, 1979, p. 102.
- [10] E. B. Rosa, "The self and mutual inductance of linear Conductors," *Bulletin Nat. Bureau Standards*, vol. 4, pp. 301-344, 1908.
- [11] A.R. Djordjević and T. K. Sarker, "Closed-Formulas For frequency Dependent Resistance and Inductance and Strip Transmission Lines", *IEEE transactions on microwave theory and techniques*, vol. 42, no. 2, February 1994.
- [12] S. Ramo, J. R. Whinnery, and T. V. Duzer, *Fields and waves in communication electronics*, New York: John Wiley & Sons, 1994.
- [13] N. S. Nahman and D. R. Holt, "Transient analysis of coaxial cables using the skin effect approximation $A+B s^{-1/2}$," *IEEE Transactions on Circuit Theory*, Vol. 19, pp. 443-451, 1972.
- [14] L. C. Calvey and J. L. Bihan, "Coefficient algorithm for time-domain response of skin effect lossy coaxial cables with arbitrary resistive terminations," *IEEE Trans. On Circuit and Systems*, vol. 9, pp. 915-920, Sept. 1986.